PREDICTION OF SORGHUM BIOMASS BASED ON IMAGE BASED FEATURES DERIVED FROM TIME SERIES OF UAV IMAGES

Zhou Zhang, Ali Masjedi, Jieqiong Zhao and Melba M. Crawford

Dept. of Civil Engineering, Purdue University, USA
E-mail: zhan1553@purdue.edu; amasjedi@purdue.edu; zhao413@purdue.edu; mcrawford@purdue.edu

ABSTRACT

High throughput plant phenotyping has gained significant interest in the plant science community due to its potential impact in advancing the use of advanced plant genetics for problems ranging from global food security to biomass-based energy crops. While traditional collection of field-based phenotypes is manual, automated remote sensing-based methods can reduce the manual requirements, expand the number of sampled points, and accelerate associations with genotypes. In this preliminary work, we use multiple types of features derived from multi-temporal UAV-based hyperspectral and RGB image data for prediction of sorghum biomass. Considering the nonlinear properties of the spectral input features, multiple layer perception (MLP) neural networks and support vector regression (SVR) are explored for predicting dry biomass. The analysis is conducted on datasets acquired during June-August 2016 over an agricultural test field at the Agronomy Center for Research and Education (ACRE) at Purdue University.

Index Terms— Automated phenotyping, regression, hyperspectral data, RGB images

1. INTRODUCTION

Plant phenotyping refers to quantification of the effects of the measurable characteristics (e.g.. plant height, leaf counts, and biomass). While plant genomes can now be sequenced, the relationship between phenotypes and genotypes is not well understood. The relationship is often represented as P=G X E X M, where phenotypes are related to genotypes, environmental conditions (E) and management practices (M). Traditional phenotyping is based on manual data collection, which is extremely time consuming and laborious, thereby limiting observations and thus ultimately in relating phenotypic information to genomic data. Automated image-based phenotyping approaches for field crops have become popular with plant breeders [1], [2]. These approaches are non-destructive and non-invasive and can help accelerate the linkage of associations with genotypes, thereby leading to reduced breeding cycles for acquisition of desired traits. Unmanned aerial vehicles (UAVs) have recently become relevant for plant phenotyping because of their capability to acquire high spatial resolution data with accurate positioning "on demand" when weather conditions are favorable – potentially resulting in high temporal resolution data sets throughout the critical times of the growing season [3].

Remotely sensed data from sensing modalities can provide complementary information for phenotypic analysis. For example, leaf counts and plant heights are geometrically based and can be derived from high resolution RGB data, while the chlorophyll content is related to spectral reflectance features. Although combining multi-sensor, multi-temporal data can typically increase prediction accuracy of models, significant challenges must be addressed in developing robust supervised predictive models due to the high dimensional input features and nonlinear relationships.

In this work, we investigate two nonlinear statistical learning algorithms, MLP and SVR, for prediction of dry biomass. The results and analysis provide useful insights on feature importance for prediction and demonstrate the ability of estimating the biomass from remotely sensed data.

2. DATA ACQUISITION AND FEATURE EXTRACTION

In this preliminary study, two imaging modalities: RGB and hyperspectral images acquired from UAVs were considered for feature extraction and predictive learning.

2.1. Data Acquisition

Data were acquired for 18 sorghum varieties over an agricultural sorghum field with at the Agronomy Center for Research and Education (ACRE) at Purdue University during the 2016 growing season. Fig. 1 shows the ground reference map for the field. Colored rectangles indicate 144 field plot boundaries, including 72 high density (223,000 plants/ha) plots (two columns close to the west side), and 72 low plant density (52,000 plants/ha) plots (two columns close to the east side), with 18 in the N-S direction and 8 in

the E-W direction, where twelve rows were planted in each plot.

The RGB data were collected by a Sony Alpha 7R camera with 35mm lens mounted on a DJI S1000+ multirotor platform. The Sony camera, acquired imagery at a data rate of 1 frame every 1.2 seconds from a flying height of 55m, with the platform moving at a speed of 10 m/s. The camera was operated with a full resolution of 35 megapixels (7360-by-4912 pixels/image), resulting. in a GSD of ~ 0.75cm. The hyperspectral data were acquired by a Headwall Nano-Hyperspec push-broom scanner with a 12mm lens onboard a fixed-wing UAV platform. The system collected 272 bands at ~2.2nm spectral resolution and 640 pixels per scan line, operating at a scan rate of 230 lines/s. Navigation data were acquired by an Xsense MTi-G-700 GPS/IMU unit attached to the camera. The UAV was flying at a speed of 13m/sec at ~100m altitude . The corresponding GSD for this flight configuration was ~6cm.

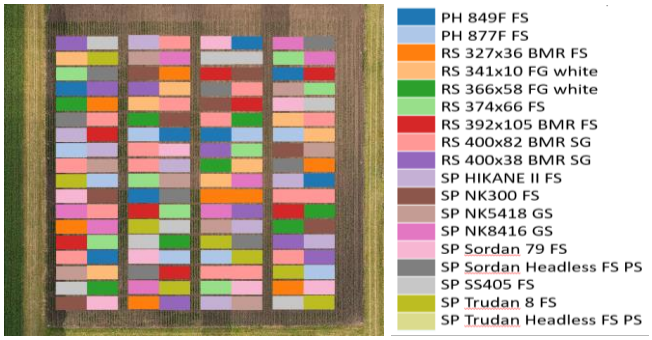

Fig. 1. Ground reference map for the sorghum field.

2.2. Feature Extraction

Disparate features from both RGB and hyperspectral images were extracted at the plot level including:

(1) Plant height histogram: photogrammetrically based height maps were generated from the RGB images through dense matching [4]. Plant heights were then obtained by comparing the derived geospatial coordinates over time. Fig. 2 shows the height difference map obtained on 07/15/2016 relative to the height map derived from 06/24/2016 heights. Brighter colors represent greater growth between these dates. The high density plants are generally taller than low density plants. To capture the height distribution in each plot, the histogram was computed for each plot using 25 equally spaced bins. The counts were normalized to sum to one [5]. The histogram of the plant height is shown in Fig. 3 for one variety (SP SS405 FS) across the growing season. The figures clearly show the plant growth patterns differ. Other RGB-based features were considered, including leaf counts, but did not improve predictions.

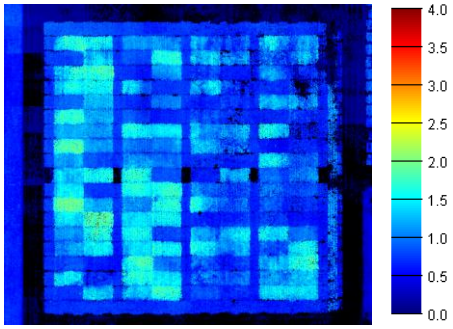

Fig. 2. Height difference map for the sorghum field on 07/15/2016

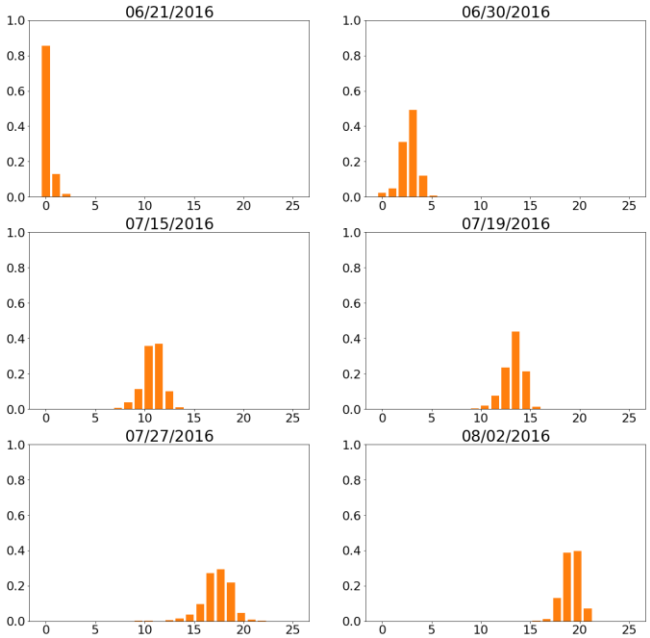

Fig. 3. Histograms of incremental growth in SP SS405 FS sorghum relative to 06/24

(2) Spectral features: the hyperspectral data were geometrically and radiometrically corrected. For the geometric correction, the data were orthorectified in a two stage process, first using the Headwall SpectralView software based on the GPS/IMU data from the Xsense, and then fine-tuned by co-registering to the RGB based orthophoto [6]. The raw hyperspectral data were first converted to radiance using SpectralView then calibrated to reflectance using FLAASH. Shadows and data from noisy bands beyond 900nm were removed. The mean spectrum over the entire plot was used to represent the plot spectral information, and the spectral feature vector includes 113 bands. Fig. 4 shows the true color composite of the hyperspectral data (left) collected on July 11, 2016, and the mean spectrums for three plots (right).

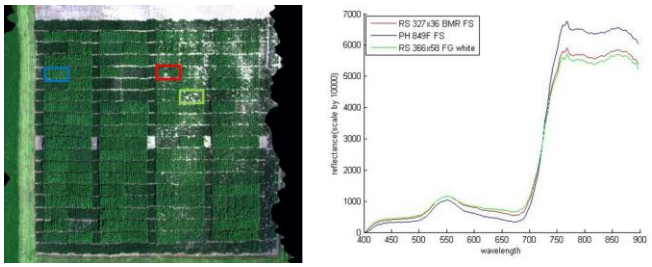

Fig. 4. True-color composite of the hyperspectral data (left) and plot level spectrums (right).

(3) Spectral indices: spectral indices are very useful for analysis of the health of vegetation. Multiple hyperspectral indices were explored, including: (a) SR705=R_{750}/R_{705}, (b), ND705=$(R_{750}-R_{705})/(R_{750}+R_{705})$, (c) mSR705=$(R_{750}-R_{445})/(R_{705}-R_{445})$, (d) mND705=$(R_{750}-R_{705})/(R_{750}+R_{705}-2R_{445})$, (e) NDVI=$(R_{800}-R_{670})/(R_{800}-R_{670})$, where SR represents simple ratio and ND represents normalized difference. mSR705 (mND705) is a modified version of SR705 (ND705). R_{445} was subtracted from all reflectance values to compensate for specular reflectance. We used the mSR705 index in the models, as yielded good results for our data.

3. METHODOLOGY

To predict the biomass using the derived features from both RGB and hyperspectral data, nonlinear models are preferred since linear models are unable to characterize the nonlinear scattering phenomena. Two nonlinear regression models were developed, Support Vector Regression (SVR) and Multi-Layer Perception (MLP).

In the remote sensing community, Support Vector Machines (SVM) have been demonstrated to be effective for classification. SVR is similar to SVM but focused on predictive models [8]. A Gaussian radial basis function kernel $K(\mathbf{x}_i,\mathbf{x}_j)=\exp(-\gamma\left\|\mathbf{x}_i-\mathbf{x}_j\right\|^2)$ was adopted, where γ was the width of the kernel function. Using this kernel, the input data are mapped into a low dimensional space where a linear regression can fit the data, Overfitting was avoided by using a regularizer on the estimated coefficients. The kernel parameter γ and the regularizer weighting parameter were tuned through cross validation during the training process.

Multi-Layer Perceptron (MLP) is an artificial neural network with one or more hidden layers of neurons. It is capable of modelling highly nonlinear functions between the input and output. It forms the basis of deep-learning neural network (DNN) models, and has been widely used in hyperspectral data applications [9]. The MLP model is typically trained in three phases, 1) *forward phase*, the input features are incorporated into the network, and computations across layers are conducted using the current set of weights, 2) *backward phase*, the error between the ground reference data and the predicted values at the output layer is computed and propagated successively back through the network to update the weights. In this study, a five layer MLP model was designed, with one input layer, three hidden layers and one output layer. (See Fig. 5). In the input layer, the number of neurons was equal to the number of input features, and the output layer had only one neuron, which represented predicted dry biomass. For the three hidden layers, the numbers of neurons were experimentally set to 512, 256 and 8.

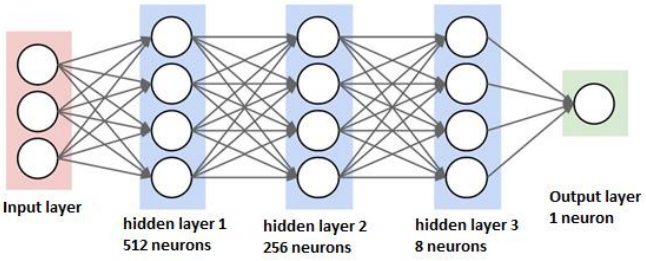

Fig. 5. Proposed MLP architecture for biomass prediction.

4. EXPERIMENTAL RESULTS

4.1. Experimental Design

Experiments were conducted on 72 high density plots, containing 18 varieties with 4 replicates. The ground reference measurements for dry biomass were collected on 08/04. Features were extracted from a time series of UAV image data, including 1) hyperspectral data acquired on 06/24, 07/11, and 08/04, and 2) RGB data acquired on 06/21, 06/30, 07/15, 07/19, 07/27, and 08/02. Different combinations of features at multiple-times were explored for biomass prediction. Table 1 contains details for each experiment. We randomly partitioned the 72 plots and used 4-fold cross validation to evaluate the performance of our models. Four rounds of experiments were conducted, such that, 54 plots were used for training and 18 plots were used for testing in each round.

4.2. Results and Analysis

The SVR and MLP models were trained as described in Section 3, and ten experiments were conducted with different input features as shown in Table 1. The averaged results from the four-fold cross-validation are listed in Table 2. Root mean square error (RMSE) and R^2 were used to evaluate the model predictions. The results show that Exp 4-10 in general have better performance than Exp 1-3, indicating that combining height and spectral data improved the prediction ability, although the model based on 7/11 spectral data had about the same predictive capability. Also, the R^2increased as more features from multiple dates were incorporated, especially for the SVR model. Interestingly,

Table 1 Experimental design with different combinations of input features

# Exp	Spectral Features+Spectral Index	Height Histogram
1	06/24	--
2	07/11	--
3	08/04	--
4	06/24	06/21
5	07/11	06/21+06/30
6	08/04	all six dates
7	06/24+07/11	06/21+06/30
8	06/24+08/04	all six dates
9	07/11+08/04	all six dates
10	06/24+07/11+08/04	all six dates

Table 2 Biomass prediction accuracies for different experiments

# Exp	SVR		MLP	
	RMSE (g/m^2)	R^2	RMSE (g/m^2)	R^2
1	205.28	0.48	213.83	0.43
2	179.33	0.58	180.36	0.60
3	265.17	0.13	274.88	0.04
4	220.44	0.46	239.00	0.37
5	187.42	0.61	188.40	0.61
6	178.89	0.65	199.19	0.55
7	174.11	0.66	188.60	0.61
8	161.31	0.71	188.38	0.61
9	155.41	0.73	184.15	0.62
10	148.02	0.76	196.30	0.57

we see that the SVR model in general performs better than the MLP model. This is likely because the ground reference data for biomass were extremely limited, and the large number of weighting parameters associated with the high dimensional features could not be properly learned. To further investigate the MLP model, learning curves for the loss function, training accuracy and the testing accuracy are shown in Fig. 6. As the number of iterations grows, the training accuracy also increases, while the testing accuracy increases first and then decreases, which clearly shows that overfitting occurred in the training phase.

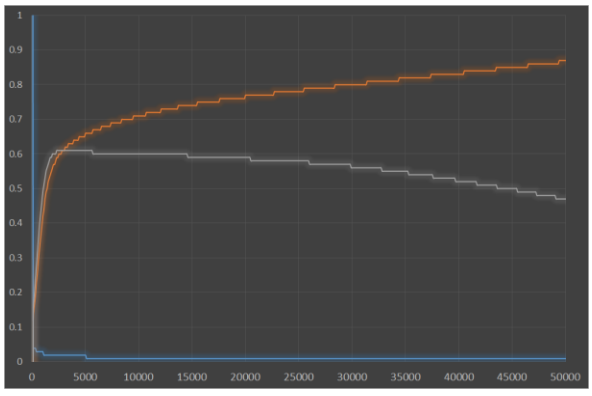

Fig. 6. Learning curves for of MLP for Exp 10;
loss error; training acc; testing acc;

5. CONCLUSIONS

Two nonlinear regression models were developed to predict sorghum biomass using remotely sensed data from UAV. Experimental results show that combining spectral and height features and multiple dates can result in better prediction performance than using either a single type of feature or features from a single date. However, due to the limited quantity of ground reference data, the performances of the models were suboptimal, especially for MLP, as it typically requires a large quantity of training samples to learn the optimal weights. We are investigating data augmentation strategies to generate additional training data. Data from other modalities thermal and LiDAR will also be acquired in the future, and evaluated for improving the model.

6. ACKNOWLEDGEMENT

This work was supported by the Advanced Research Projects Agency-Energy (ARPA-E), U.S. Department of Energy under Grant DE-AR0000593.

7. REFERENCES

[1] E. P. Spalding and N. D. Miller, "Image analysis is driving a renaissance in growth measurement," *Curr. Opin. Plant Biol.*, vol. 16, no. 1, pp. 100–104, 2013.
[2] L. Li, Q. Zhang, and D. Huang, "A review of imaging techniques for plant phenotyping," *Sensors*, vol. 14, no. 11, pp. 20078–20111, 2014.
[3] Y. Shi et al, "Unmanned aerial vehicles for high-throughput phenotyping and agronomic research," *PLOS One*, 2016.
[4] N. Haala and M. Rothermel, "Dense multi-stereo matching for high quality digital elevation models," *Photogrammetrie-Fernerkundung-Geoinformation*, 2012(4):331-343, 2012.
[5] K. Ramamurthy, Z. Zhang, A. M. Thompson et al, "Predictive modeling of sorghum phenotypes with airborne image features," *2016 KDD workshop on data science for food, energy and water*, Aug. 2016.
[6] A. Habib, W. Xiong, F. He et al, "Improving orthorectification of UAV-based push-broom scanner imagery using derived orthophotos from frame cameras," *IEEE J. Sel. Topics Appl. Earth Observ*. 2016.
[7] D. A. Sims and J. A. Gamon, "Relationships between leaf pigment content and spectral reflectance across a wide range of species, leaf structures and developmental stages," *Remote Sens. Environ.*, vol. 81, no. 2, pp. 337-354, 2002.
[8] Z. Pan, C. Glenni, C. Legleiter and B. Overstreet, "Estimation of water depth and turbidity from hyperspectral imagery using support vector regression", *IEEE Geosci. Remote Sens. Lett.*, vol. 12, no. 10, pp. 2165-2169, 2015.
[9] A. Baraldi, E. Binaghi, P. Blonda, P. A. Brivio and A. Rampini, "Comparison of the multilayer perceptron with neuro-fuzzy techniques in the estimation of cover class mixture in remotely sensed data," *IEEE Trans. Geoscience and Remote Sensing*, vol. 39, no. 5, pp. 994-1005, 2001.